

Influence of antidots on transport characteristics of HTSC

A.N. Moroz, A.N. Maksimova, V.A. Kashurnikov, I.A. Rudnev

NRNU MEPhI, Moscow, Russia

moroz.anna@hotmail.com



A numerical study has been conducted on the dependencies of critical current density J_c of typical high- T_c superconductors on the density and distribution of antidots – macroscopic circular regions of hollowed-out material. All computations have been carried out by using the Monte-Carlo method within the limits of the model of a layered high-temperature superconductor (HTSC). Multiple series of voltage-current characteristics of samples have been calculated for different quantities of antidots N_a as well as for different values of point defect concentration n_d . The diameter size of antidots varied from 50 nm to 2 μm . Different kinds of antidot distribution, such as square and triangular lattices and random and conformal arrays, have been considered.

The dependencies of J_c on the number of antidots with fixed diameters as well as on the diameter size with fixed number of antidots have been plotted. The results have shown that J_c grows with the increasing diameter size of antidots within the considered limits of concentrations. Average vortex configurations have been acquired for all samples in order to demonstrate the influence of antidots on the vortex lattice behavior.

Model for calculations

The Gibbs potential for a two-dimensional system of interacting vortices can be described by (1). It is composed of a sum of the vortices' own energies (2), as well as the energies of vortex-vortex (3), vortex-defect (4), vortex-surface (5), and vortex-transport and Meissner current (6) interactions.

$$G = N\varepsilon + \frac{1}{2} \sum_{i \neq j} U(r_{ij}) + \sum_{i,j} U_{\text{pn}}(r_{ij}) + \sum_{i,j} U_{\text{surf}}(|r_i - r_j|) + \sum_i U_m(x_i) \quad (1)$$

$$\varepsilon = \delta \frac{\Phi_0^2}{(4\pi\lambda)^2} \left(\ln\left(\frac{\lambda_0}{\xi_0}\right) + 0.52 \right) \quad (2)$$

$$U(r_{ij}) = \delta \frac{\Phi_0^2}{8\pi^2\lambda^2} K_0\left(\frac{r_{ij}}{\lambda}\right) \quad (3)$$

$$U_{\text{pn}}(r_{ij}) = -\alpha \left(1 + \frac{r_{ij}}{\xi}\right)^{-1} \exp\left(-\frac{r_{ij}}{2\xi}\right) \quad (4)$$

$$U_{\text{surf}}(|r_i - r_j|) = -\frac{1}{2} \delta \frac{\Phi_0^2}{8\pi^2\lambda^2} K_0\left(\frac{|r_i - r_j|}{\lambda}\right) \quad (5)$$

$$U_m(x_i) = \frac{\Phi_0}{4\pi} \left\{ H_0 \left[\cosh\left(\frac{x_i}{\lambda}\right) \left(\cosh\left(\frac{dL}{2\lambda}\right) - 1 \right) + H_1 \left[-\sinh\left(\frac{x_i}{\lambda}\right) \left(\sinh\left(\frac{L}{2\lambda}\right) \pm 1 \right) \right] \right\} \quad (6)$$

Here N is the number of vortices in the system, λ_0 and ξ_0 are the magnetic field penetration depth and the coherence length at absolute zero respectively. Their temperature dependency is as follows: $l = l_0(1 - (T/T_c)^{3.3})^{-1/2}$ where T_c is the critical temperature. The vortices' interaction with antidots was described as a vortex-surface interaction given by (5) accompanied by an interaction with point defects (4) surrounding each antidot. The recent images made with SEM showed that columnar defects appear around antidots in real samples (Figure 1). This justifies the use of point defects in our model. The system's geometry is shown in Figure 2.

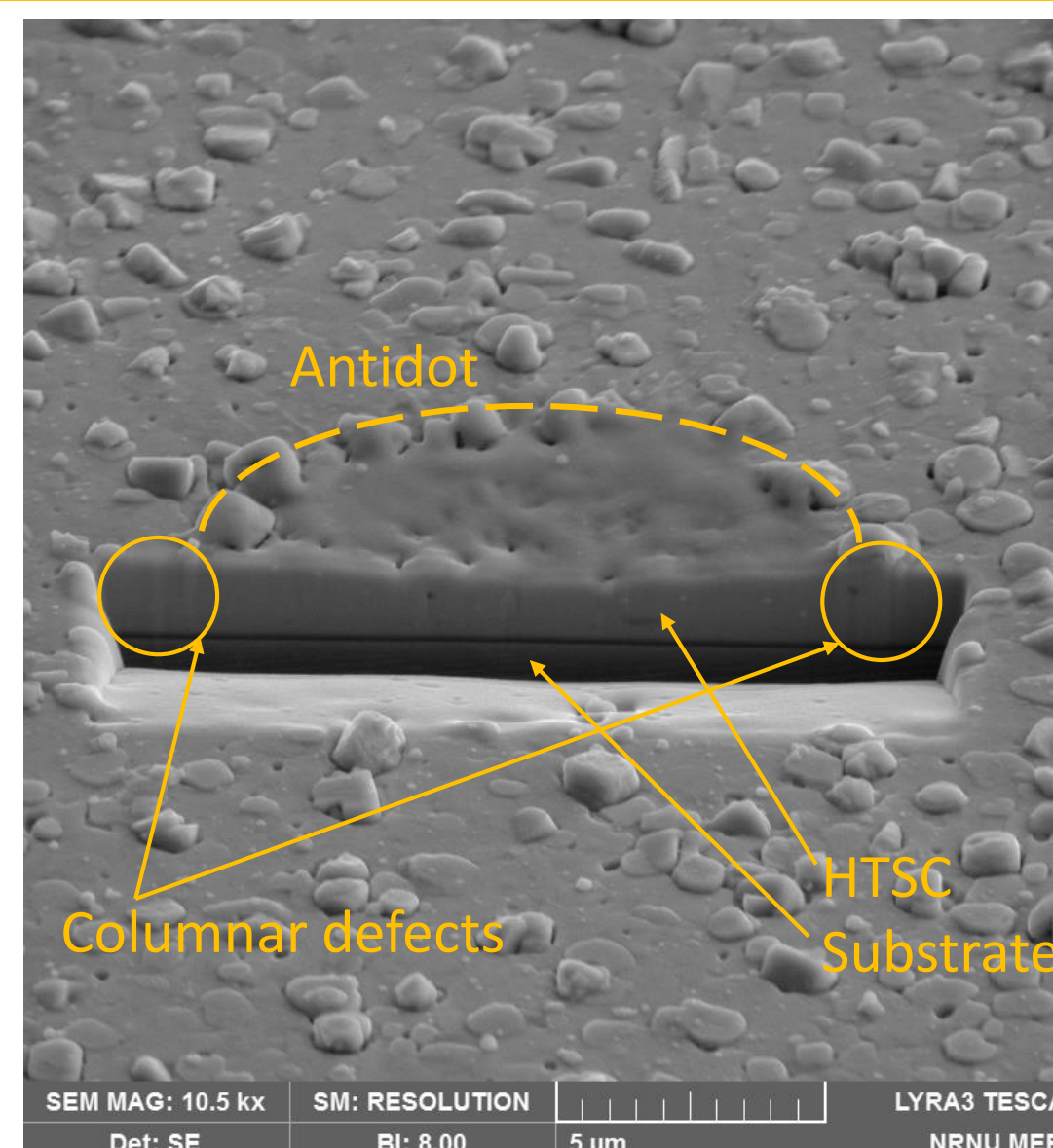


Figure 1. An image of an antidot acquired by using a Scanning Electron Microscope (SEM).

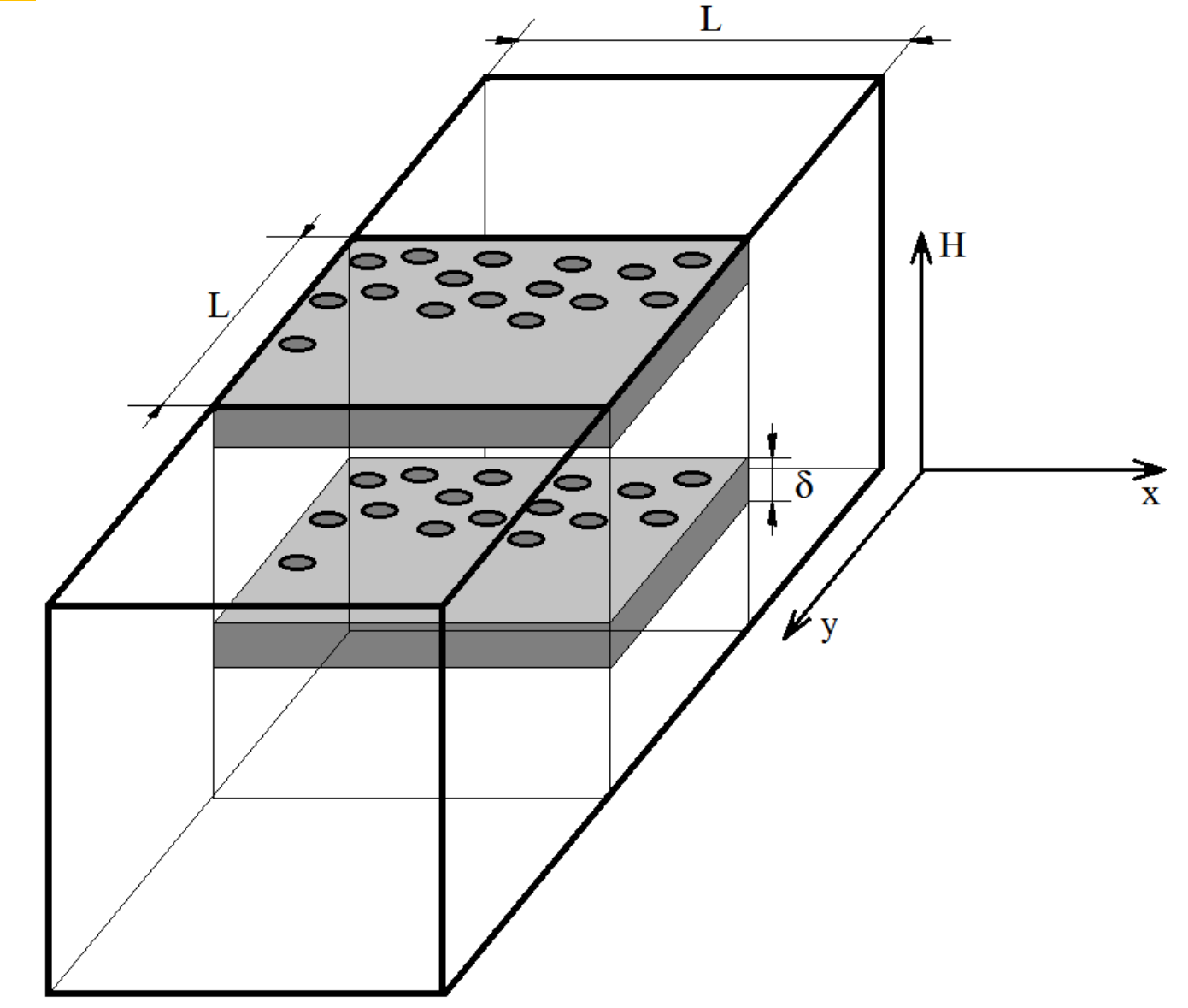


Figure 2. Geometry of computations.

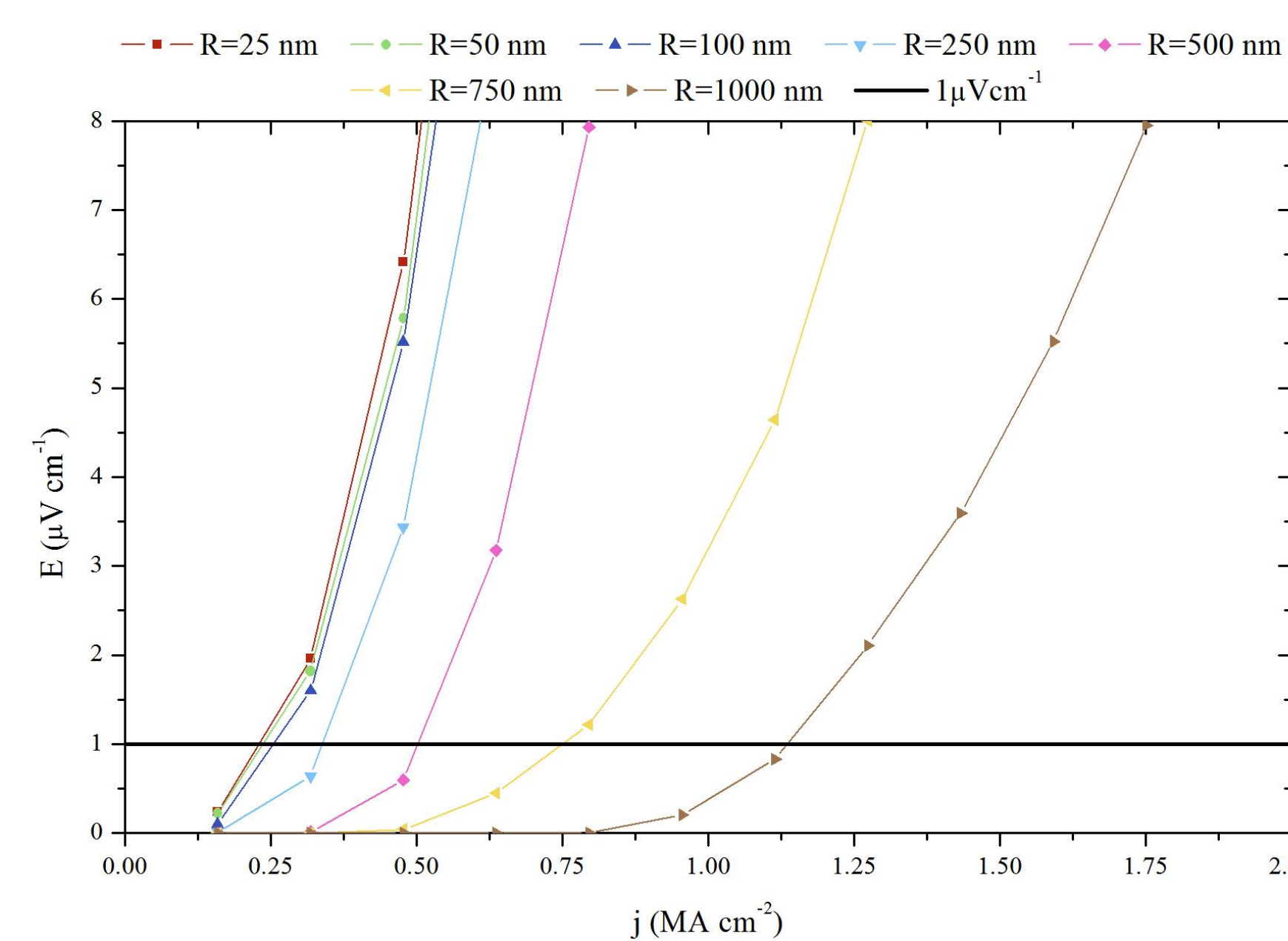


Figure 3. A series of voltage-current characteristics of a 15x15 μm sample containing 39 antidots and no additional point defects for 7 different sizes of antidots varying from 50 nm to 2 μm in diameter.

Similar voltage-current characteristics were acquired for samples with 59 and 82 antidots. In addition, two point defect concentrations were considered (500 and 1000 defects in total).

From each of the acquired voltage-current characteristics two of major transport parameters were obtained. These parameters are the critical current density j_c and the so-called n-value. j_c was determined by the standard electric field criterion of $1 \mu\text{V}/\text{cm}$. The n-value was determined from each point of its voltage-current characteristic by using the equation:

$$n = \frac{\ln\left(\frac{E}{E_c}\right)}{\ln\left(\frac{j}{j_c}\right)}$$

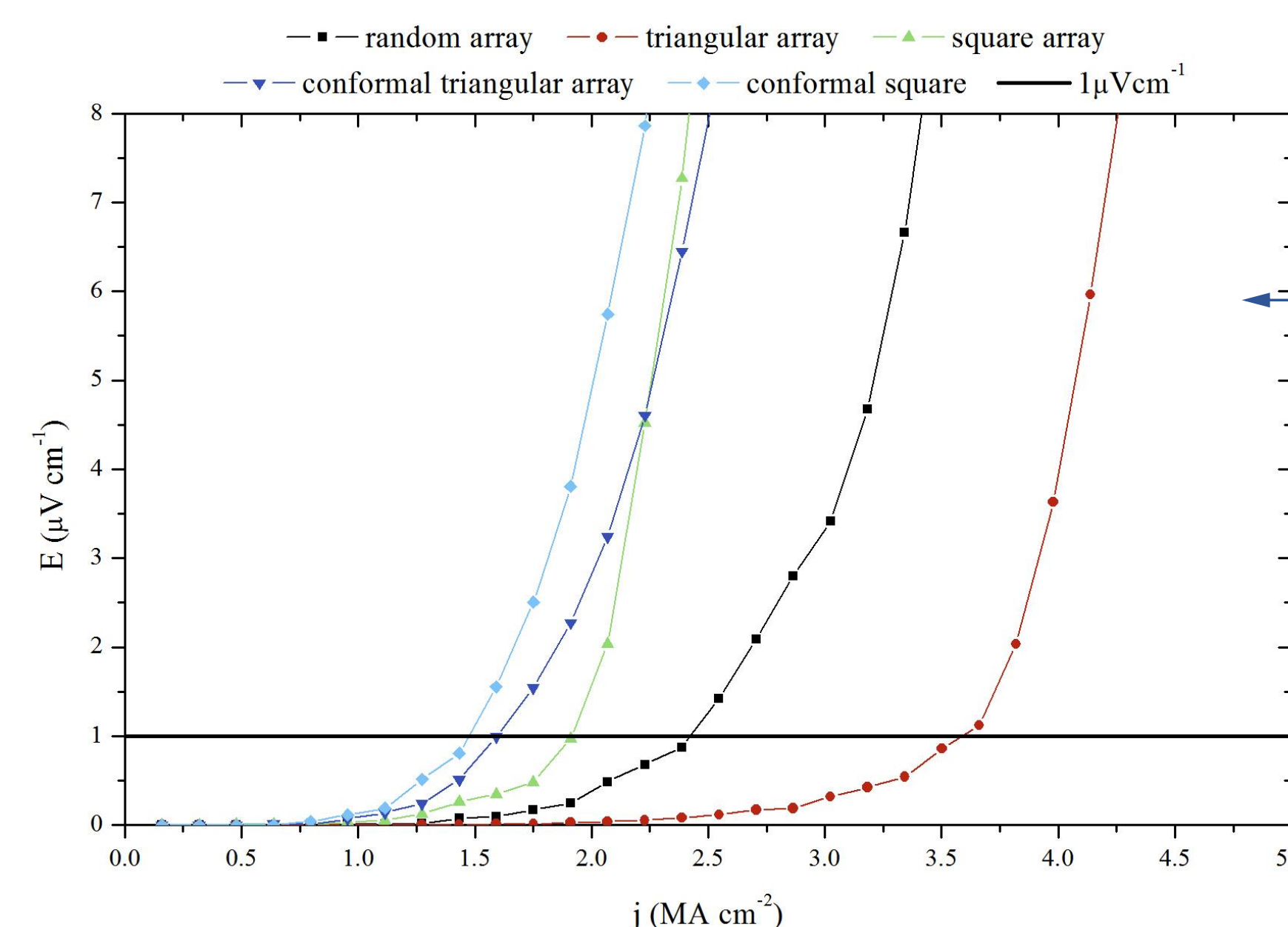


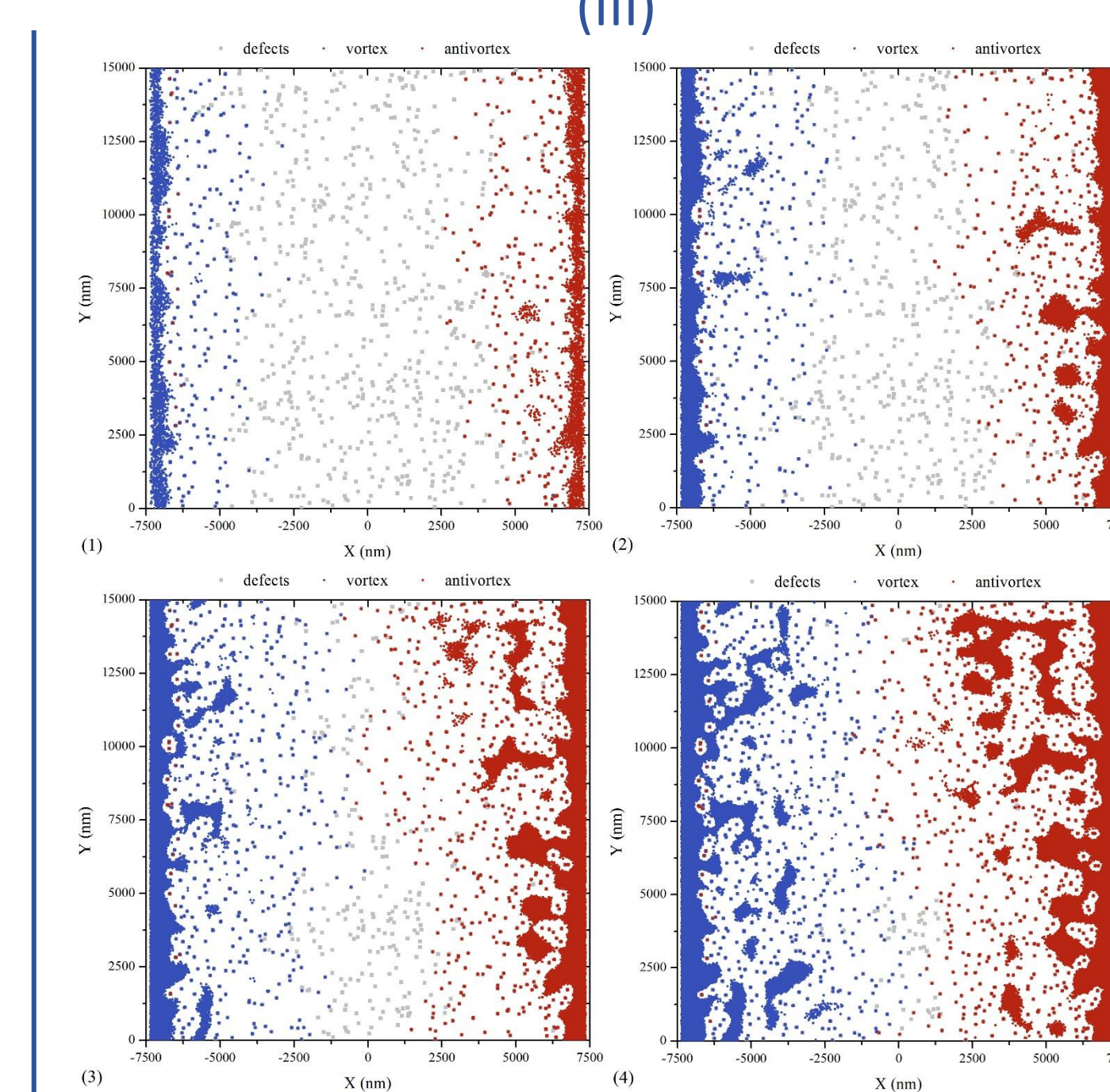
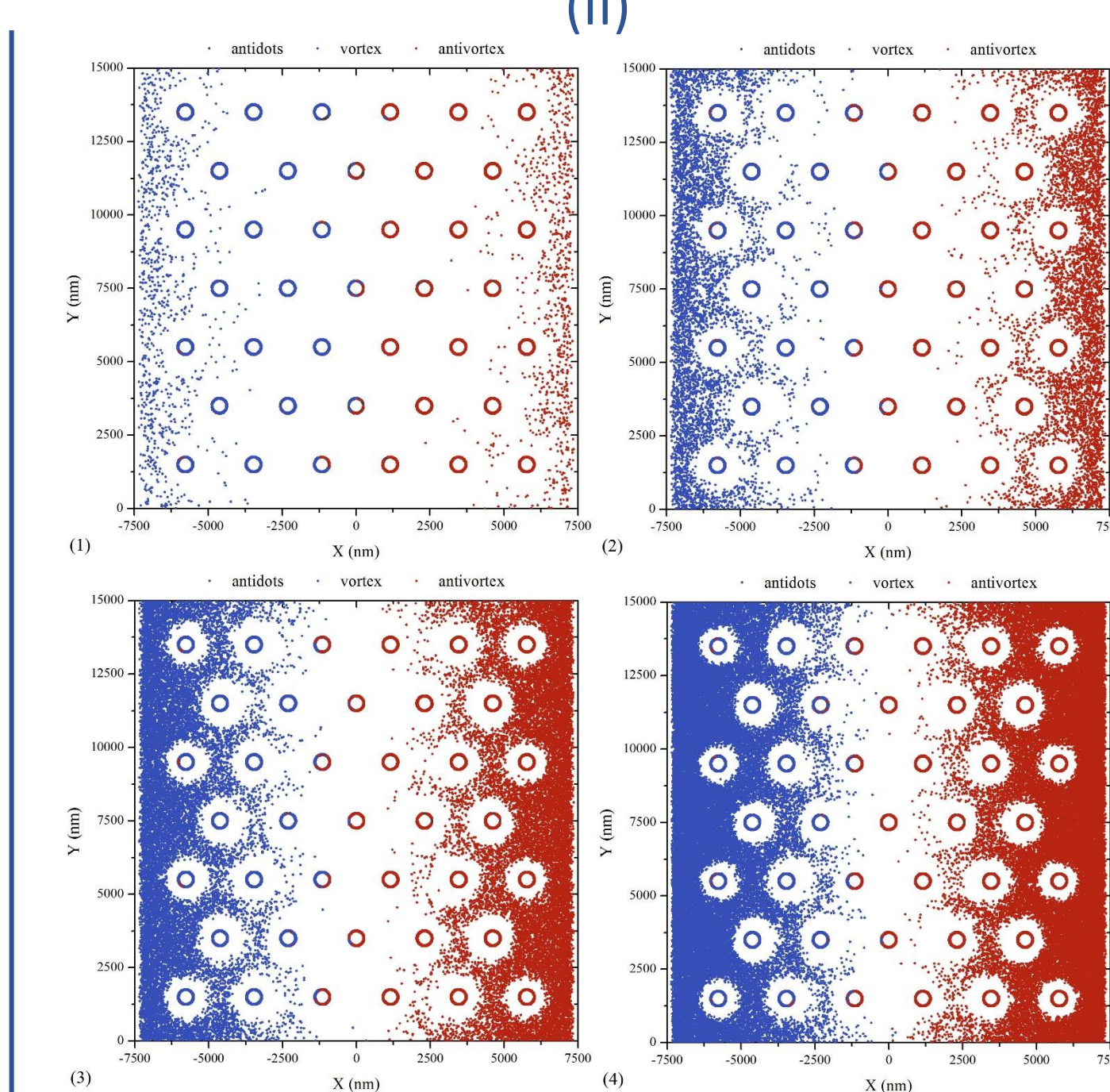
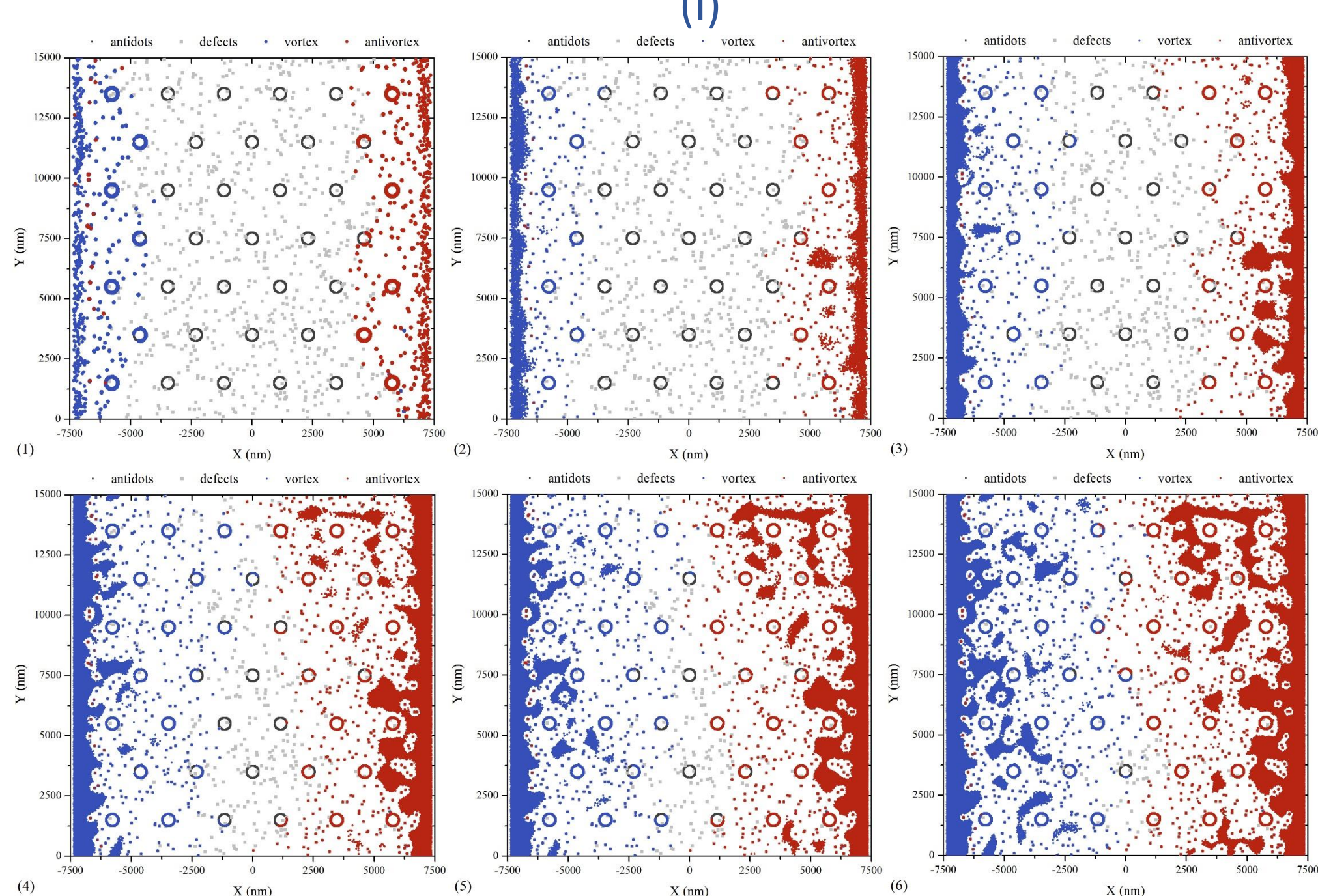
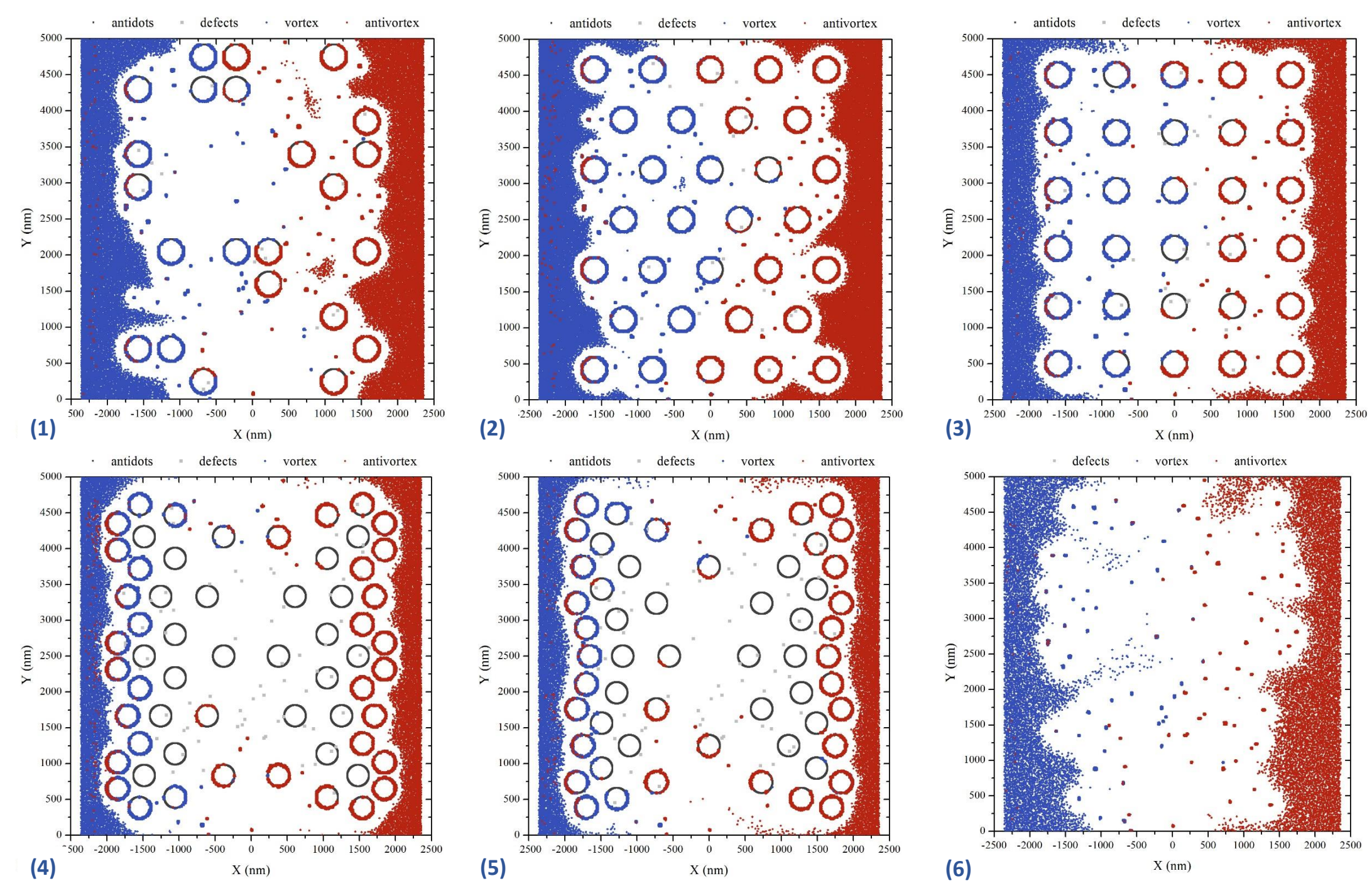
Figure 4. A series of voltage-current characteristics of a 5x5 μm sample containing 100 point defects and ~30 antidots (150 nm in diameter) in different distributions such as: random, triangular, square, conformal triangular, and conformal square arrays.

Average vortex configurations for the mentioned distributions (1-6 respectively) are shown below as well as for a sample with no antidots (6) for comparison.

Both in figures 5 and 6 it can be seen that the vortices get pinned by the antidots and point defects and the number of vortices captured by one antidot depends on its size. Unpinned vortices are pushed towards the middle of the sample by the Lorentz force and flow around the occupied antidots and point defects until they reach a vacant pinning center or find themselves trapped in a space between other pinned vortices.

Figure 4. The growing dependencies of critical current (left column) and n-value (right column) on the size of antidots (upper row), number of antidots (middle row), and number of defects (lower row).

As it can be seen, both parameters increase with the increasing R , N (antidots) and N (defects) within the considered limits of sample parameters. Furthermore, as can be seen in the bottom four pictures, the bigger the antidots, the steeper the slope of the curve.



Conclusion

A typical high-temperature superconductor has been numerically studied to determine the influence of antidots on its transport characteristics. Several series of voltage-current characteristics have been acquired for different antidot and point defect concentrations as well as for different sizes of antidots. The resulting dependencies of critical current and n-value on the before mentioned parameters showed a consistent growth.

Multiple vortex images have been acquired for different samples. The antidots appear to be acting as effective pinning sites.

Research has been done with the financial support of RSF (grant no. 14-22-00098)

Figure 5. Average vortex configurations for a sample with 39 antidots and 1000 point defects (I), 39 antidots and no point defects (II), and no antidots and 1000 point defects (III) in different points of their voltage-current characteristics.